

FIRST SCATTERED LIGHT IMAGES OF DEBRIS DISKS AROUND HD 53143 AND HD 139664

PAUL KALAS,¹ JAMES R. GRAHAM,¹ MARK C. CLAMPIN,² AND MICHAEL P. FITZGERALD¹

Received 2005 November 10; accepted 2005 December 7; published 2006 January 19

ABSTRACT

We present the first scattered light images of debris disks around a K star (HD 53143) and an F star (HD 139664) using the coronagraphic mode of the Advanced Camera for Surveys (ACS) on board the *Hubble Space Telescope* (HST). With ages of 0.3–1 Gyr, these are among the oldest optically detected debris disks. HD 53143, viewed $\sim 45^\circ$ from edge-on, does not show radial variation in disk structure and has a width >55 AU. HD 139664 is seen close to edge-on and has a beltlike morphology with a dust peak 83 AU from the star and a distinct outer boundary at 109 AU. We discuss evidence for significant diversity in the radial architecture of debris disks that appears unconnected to stellar spectral type or age. HD 139664 and possibly the solar system belong in a category of narrow belts 20–30 AU wide. HD 53143 represents a class of wide-disk architecture with a characteristic width >50 AU.

Subject headings: circumstellar matter — stars: individual (HD 53143, HD 139664)

1. INTRODUCTION

The configuration of our solar system is perhaps the most significant starting point for our understanding of planet formation. Therefore, a fundamental question is whether or not the architecture of our solar system is common relative to other planetary systems. One point of comparison is the structure of our Kuiper Belt relative to other systems, which are typically seen as debris disks in scattered light or thermal emission. In scattered light, some debris disks, such as β Pic and AU Mic, have central holes but are radially extended to radii of hundreds of AU (Smith & Terrile 1984; Kalas et al. 2004). Other debris disks, such as HR 4796A and Fomalhaut, consist of relatively narrow rings with sharp inner and outer boundaries (Schneider et al. 1999; Kalas et al. 2005). However, a narrow-belt architecture has not previously been detected in scattered light among stars similar in spectral type and age to the Sun.

HD 53143 (K1 V) and HD 139664 (F5 V) are two stars about 18 pc from the Sun known to have circumstellar dust due to excess thermal emission at far-infrared wavelengths (Aumann 1985; Stenel & Backman 1991; Table 1). Various indicators place the age of HD 53143 at 1.0 ± 0.2 Gyr (Decine et al. 2000; Song et al. 2000; Nordstrom et al. 2004), whereas HD 139664 may be a younger system with an age of $0.3^{+0.7}_{-0.2}$ Gyr (Lachaume et al. 1999; Montes et al. 2001; Mallik et al. 2003; Nordstrom et al. 2004). For these two stars the infrared excess corresponds to a dust mass 3–10 times smaller than that of ~ 10 Myr old systems such as AU Mic and β Pic (Kalas et al. 2004). Direct imaging of debris disks with masses this small is observationally challenging, but it is now feasible using the optical coronagraph in ACS.

2. OBSERVATIONS AND DATA ANALYSIS

We utilized the HST ACS High Resolution Camera (HRC) with a 1/8 diameter occulting spot to artificially eclipse each star (Table 1; Fig. 1). Five F stars were observed in consecutive orbits, as were five K stars, in order to minimize differences in the point-spread function (PSF) due to telescope thermal variations. Each PSF was subtracted using the four other stars in each set of observations. The relative intensity scaling and

registration between images was iteratively adjusted until the residual image showed a mean radial profile equal to zero intensity.

After the excess nebulosity was detected around HD 53143 and HD 139664, we determined that no surface brightness asymmetries were detected between each side of each disk. To improve the signal-to-noise ratio, we mirror averaged the data (Figs. 2 and 3). Mirror averaging splits the image into two halves along the axis that is perpendicular to the disk midplane and bisects the disk. One side is transposed onto the other side and the data are then averaged. Asymmetries due to scattering phase function effects will be co-added (Kalas & Jewitt 1996). In effect, mirror averaging doubles the integration time spent on the circumstellar disk given that the broad features between each side are symmetric. As a test, we also subtracted the two disk halves from each other and confirmed that the assumption of symmetry is valid.

3. RESULTS

The two disks have different morphologies due to different inclinations and intrinsically different architectures. To quantify the viewing geometries and structural properties of the disks, we produce a series of simulated scattered light disks that explore the parameters of inclination to the line of sight, the inner and outer disk radii, and the radial and vertical variation of dust number density (Fig. 2; Kalas & Jewitt 1996). We reinsert the simulated disks across each star in a direction orthogonal to the observed midplanes and select those models that most closely resemble the properties of the observed disks. Table 1 summarizes our findings.

The shape of the midplane surface brightness distribution differs significantly for each system (Fig. 3). The HD 53143 midplane surface brightness decreases monotonically with projected radius approximately as r^{-3} , where r is the projected radius. In the simulated disk, the radial number density distribution decreases as q^{-1} , where q is radius in the disk cylindrical coordinate system. Our solar system's zodiacal dust complex has a comparable dependence of grain number density as a function of radius ($q^{-1.34}$; Kelsall et al. 1998), controlled mainly by the force of Poynting-Robertson (PR) drag that causes small grains to spiral into the Sun (Burns et al. 1979). Therefore, the HD 53143 disk may simply represent a population of unseen parent bodies that collisionally replenish dust that is redistrib-

¹ Department of Astronomy, University of California at Berkeley, 601 Campbell Hall, Berkeley, CA 94720.

² NASA Goddard Space Flight Center, Code 681, Greenbelt, MD 20771.

TABLE 1
STAR AND DISK PROPERTIES

Property	HD 53143	HD 139664
Star		
Age (Gyr)	1.0 ± 0.2	$0.3^{+0.7}_{-0.2}$
Spectral type	K1 V	F5 IV-V
Mass (M_{\odot})	0.8	1.3
T_{eff} (K)	5224	6653
Luminosity (L_{\odot})	0.7	3.3
Distance (pc)	18.4	17.5
m_V (mag)	6.30	4.64
Disk		
Peak disk surface brightness (mag arcsec $^{-2}$)	22.0 ± 0.3	20.5 ± 0.3
Disk position angle (deg)	147 ± 2	77 ± 0.5
Inclination (deg)	40–50	85–90
Disk number density gradients (q^{β})	-1	+3.0 and -2.5
Inner dust depletion (AU)	<55	83
Maximum outer radius (AU)	>110	109
Optical depth from <i>IRAS</i> data ^a	2.5×10^{-4}	0.9×10^{-4}
Optical depth from <i>HST</i> data ^b	$>1.6 \times 10^{-5}$	1.0×10^{-5}
Total dust mass ^c (g)	$>7.1 \times 10^{23}$	5.2×10^{23}

^a The fractional dust luminosity (Zuckerman & Song 2004).

^b Derived from the model disks. Since the disks are optically thin, we sum the cumulative light from the model disk, m_d , and quote optical depth as $10^{(m_d - m_V)/-2.5}$. We assume an albedo of 1 and that the optical depth will scale inversely with the assumed albedo.

^c Dust mass follows from the *HST* optical depth and assumes a uniform particle radius of 30 μm , a density of 2.5 g cm $^{-3}$, and an albedo of 1.0.

uted radially by PR drag. Our simulations show that the outer radius of the observed disk is a sensitivity-limited value of approximately 6'' (110 AU). The inner radius is also sensitivity limited, to 3'' (55 AU). Therefore, the debris disk around HD 53143 is at least 55 AU wide.

Material surrounding HD 139664, on the other hand, is confined to a narrow belt, as indicated by a turnover in the midplane surface brightness profile between 4'' and 5''.5 (79–96 AU; Fig. 3). Our disk simulations show that the peak in the dust distribution occurs at 83 AU, decreasing as $q^{-2.5}$ from 83–109 AU, with a sharp outer truncation at 109 AU (Figs. 2 and 3). We tested model disks that have outer radii >109 AU and found that these disks would have been detectable in our data with radii as great

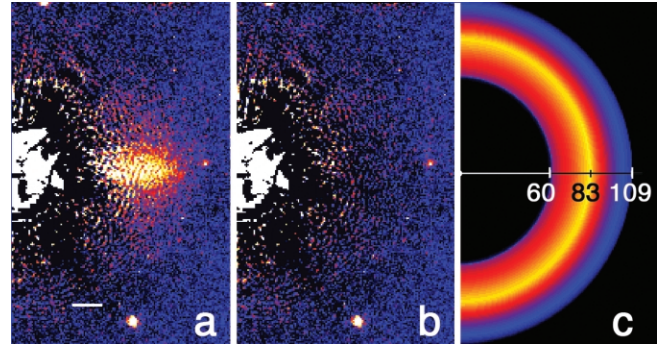


FIG. 2.—(a) Mirror-averaged image of HD 139664. The white bar has a length of 1'', and the right tip is located at 3'' radius from the star (the radius where we begin making measurements of disk properties). (b) The same data after a model disk has been subtracted. Measurements of the PSF residual along the disk midplane are now indistinguishable from all other position angles, and we consider the model a satisfactory fit to the data. Model disks with inclination range $i = 85^{\circ}$ – 90° fit the observed morphology and midplane surface brightness. This range of inclinations is allowed because a vertically fat, edge-on ($i = 90^{\circ}$) disk can have isophote morphology that resembles a vertically thin disk with $i = 85^{\circ}$. (c) Illustration of the narrow-belt architecture by inclining the model HD 139664 disk to face-on. Model properties are discussed in Fig. 3. The dust-free hole within 60 AU must be confirmed by future observations. Summing the light between the 82 and 84 AU radii in our face-on model disk, we obtain $m_{\lambda} = 20.3$ mag. The perpendicular optical depth is approximately $10^{[(4.6 - 20.3)/-2.5]} = 5.2 \times 10^{-7}$ for albedo = 1.

as 10'' (175 AU; Fig. 3). Given an absence of significant gas, the beltlike nature of HD 139664 is most likely a structure related to planet formation. Kenyon & Bromley (2004) find that a dust belt with peak surface brightness at a radius of ~ 80 AU forms within a planetesimal disk at an age of 400 Myr. The appearance of this belt signals the recent formation of a ≥ 1000 km planet that gravitationally stirs planetesimals in its vicinity. Liou & Zook (1999) and Moro-Martín & Malhotra (2002), on the other hand, simulate the concentrations of dust in trans-Neptunian space that arise due to trapping in mean-motion resonances. A natural explanation for the beltlike morphology of HD 139664 is that the ~ 83 AU peak in the dust distribution corresponds to either an interior or exterior mean-motion resonance created

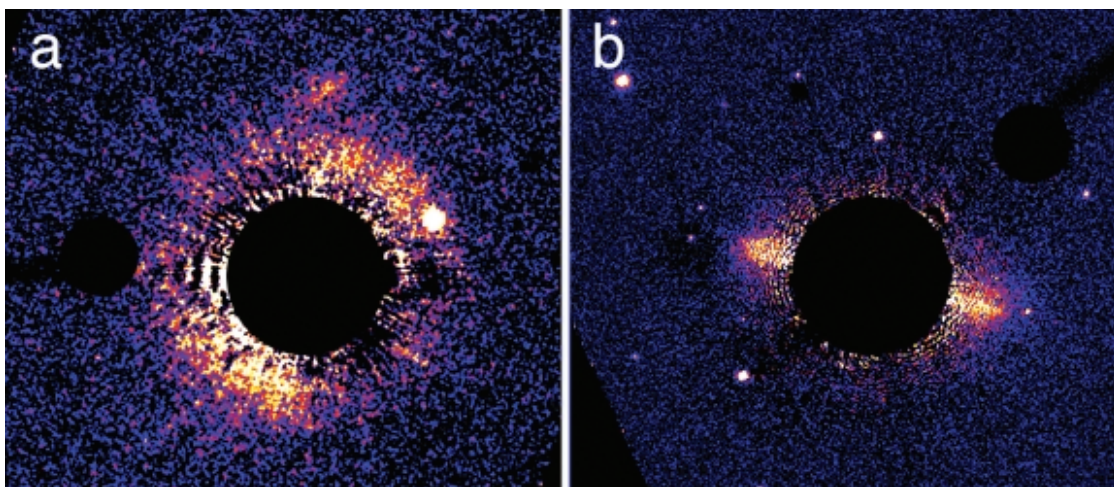


FIG. 1.—False-color ACS HRC F606W ($\lambda_c = 591$ nm, $\Delta\lambda = 234$ nm) images of scattered light from debris disks surrounding (a) HD 53143 and (b) HD 139664. North is up, east is left, and the circular black mask in each image has a radius of 3''. The periphery of each field also shows the 3'' diameter circular occulting mask located at the tip of an occulting bar. Cumulative integration times are 2340 and 2184 s for HD 53143 and HD 139664, respectively. HD 53143 and HD 139664 were observed on 2004 September 11 and October 14, respectively. The stellar full-width at half-maximum is 63 mas. The images are corrected for distortion and have 25 mas pixel $^{-1}$.

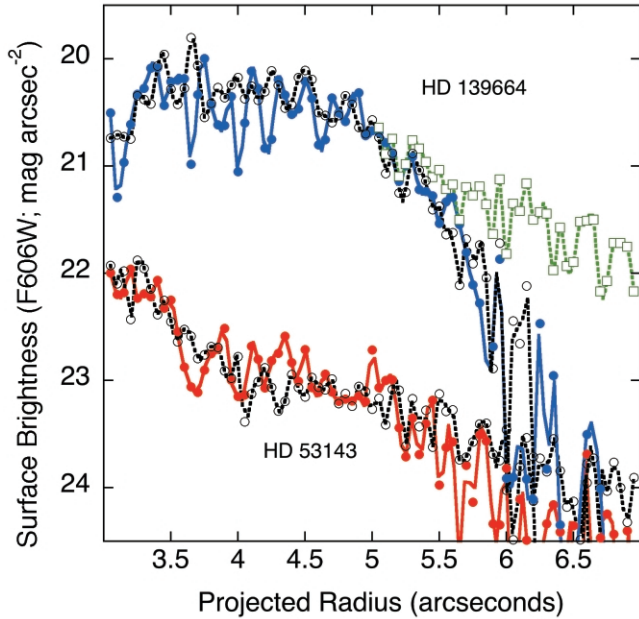


FIG. 3.—Radial surface brightness distribution along the HD 53143 and HD 139664 disk midplanes. Filled circles and solid lines trace the observed disk midplanes, and open circles and dashed lines trace model dust disks inserted into the data orthogonal to the real midplane direction. The real and model disk midplanes were sampled in a strip $1''.25$ wide for HD 53143 and $0''.25$ wide for HD 139664. The noise is indicated by the scatter of data points. A turnover in surface brightness between $4''.5$ and $5''.0$ (79 – 88 AU) is common to all PSF subtractions of HD 139664 (filled blue circles). If the HD 139664 disk extended radially inward, then the surface brightness profile should be continuously brighter inward. In order to match the midplane profile, the model disk (open black circles) has no dust within a $3''.40$ radius (59.5 AU). Between $3''.40$ and $4''.75$ (59.5 – 83.1 AU), the dust density increases as $q^{+3.0}$. Between $4''.75$ and $6''.25$ (83.1 – 109.4 AU), the dust number density decreases as $q^{-2.5}$. The model disk has no dust beyond 109.4 AU. For comparison, a model disk (open green squares) with an outer radius twice that of the best-fit case would be detected as far as a radius of $10''$. The models for HD 54143, on the other hand, do not indicate significant variations in radial structure between the detection limits of $3''$ – $6''$. All models assume isotropic scattering with scaling parameters similar to those used for β Pic by Kalas & Jewitt (1995).

by a companion to HD 139664. Large grains may dominate the belt's peak at 83 AU, with smaller grains passing quickly through the resonance regions due to radiation forces.

4. DISCUSSION

Taking a census of eight debris disks resolved in scattered light and the predicted dust distribution in our Kuiper Belt, we observe two basic architectures that are not correlated with stellar mass and luminosity, but must depend on other environmental factors (Table 2). Debris systems are either narrow belts or wide disks. Both types have central dust depletions, but the distinguishing characteristic is the presence or absence of a distinct outer edge. HR 4796A, Fomalhaut, HD 139664, and the Sun are examples of narrow-belt systems. The belt systems appear to have radial widths ranging between 20 and 30 AU, and the inner edges may begin as close as 25 AU (Sun), or as far as 133 AU (Fomalhaut). HD 32297, β Pic, HD 107146, HD 53143, and AU Mic are examples of disks with sensitivity-limited outer edges that imply disk widths >50 AU.

The F, G, and K stars are interesting because a priori we might expect to find planetary systems similar to our own, yet we discover significant diversity in the outer regions that correspond to Neptune and our Kuiper Belt. With an age of

TABLE 2
DEBRIS DISK ARCHITECTURES FROM SCATTERED LIGHT PROPERTIES

Name	r_{in} (AU)	r_{out} (AU)	Width (AU)	d (pc)	Spectral Type	References
Width > 50 AU						
β Pic	~ 90	>1835	>1745	19.3	A5 V	1, 2
HD 32297	<40	>1680	>1640	112	A0	3, 4
AU Mic	~ 12	>210	>198	9.9	M1 Ve	5, 6
HD 53143	<55	>110	>55	18.4	K2 V	7
HD 107146	~ 130	>185	>55	28.4	G2 V	8
Width = 20 – 30 AU						
HD 139664	83	109	26	18.5	F5 V	7
Fomalhaut	133	158	25	7.7	A3 V	9
HR 4796A	60	80	20	67.1	A0 V	10
Sun ^a	25	50	25	...	G2 V	11, 12

NOTES.—We do not include systems younger than 10 Myr that are likely to possess significant primordial circumstellar gas. The second column gives the inner disk radius corresponding to the approximate peak of dust number density, and the third column gives the outer radius.

^a From simulations of relatively large grains trapped in resonances with Neptune.

REFERENCES.—(1) Pantin et al. 1997; (2) Larwood & Kalas 2001; (3) Schneider et al. 2005; (4) Kalas 2005; (5) Krist et al. 2005; (6) Kalas et al. 2004; (7) this work; (8) Ardila et al. 2004; (9) Kalas et al. 2005; (10) Schneider et al. 1999; (11) Liou & Zook 1999; (12) Moro-Martín & Malhotra 2002.

~ 1 Gyr, HD 53143 is among the oldest known extrasolar debris disks, yet its wide-disk architecture resembles that of the ~ 10 Myr old systems of β Pic and AU Mic. The lingering dust mass (Table 1) throughout the system could signal the absence of giant planets that otherwise sweep clear the parent bodies (comets and asteroids) responsible for producing the dust disk. Yet the presence of a dust disk out to a radius of at least 110 AU shows that the primordial circumstellar disk probably contained the prerequisite mass of gas and dust to form giant planets. By contrast, the younger system HD 139664 has already developed a narrow-belt architecture.

Narrow-belt architectures for the underlying population of planetesimals may originate from early stochastic dynamical events, such as a close stellar flyby, that strip disk mass and dynamically heat the surviving disk (Ida et al. 2000; Adams & Laughlin 2001). Theoretical simulations show that a reduction in disk mass, combined with dynamical heating, produces a less stable planetary system that is more likely to eject giant planets from their formation site to much larger radii, as has been proposed for the origin of Neptune (Thommes et al. 1999; Tsiganis et al. 2005). Therefore, planetesimal belts not only evolve into narrow structures because of external stochastic events, but they may be found at large distances from the central star due to the subsequent outward migration of interior planets.

The collisionally replenished dust population will spread away from any narrow belt of planetesimals. If the scattered light appearance continues to manifest a narrow structure, then both the inner and outer edges are probably maintained by other gravitational perturbers such as stellar or substellar companions. However, only HR 4796 has a known stellar companion that may truncate the outer radius of the dust belt (Augereau et al. 1999). If there is no confinement mechanism for the outer radius, then the architecture will manifest as a wide disk. For example, β Pic and AU Mic may have narrow belts of planetesimals (Augereau et al. 2001; Strubbe & Chiang 2005), but the observed dust disk widths extend to hundreds of AU. Although the predicted structure of our Kuiper Belt places the solar system among the narrow-disk architectures, it is conceivable that the dust component extends to greater radii (Tru-

jillo & Brown 2001). Thus the Sun's classification as a narrow-disk system is tentative.

5. SUMMARY

We present the first optical scattered light images of debris disks surrounding relatively old main-sequence F and K stars. Material around HD 139664 is concentrated at a radius of 83 AU, with a distinct outer edge at 109 AU and a depleted, but not empty, region at <83 AU. Dust surrounding HD 53143 has a monotonic q^{-1} variation in grain number density, and the disk

edges from 55 to 110 AU are sensitivity-limited values. The different radial widths appear consistent with a more general grouping of debris disks into either narrow or wide architectures. These two categories are probably an oversimplification of significant diversity in the formation and evolution of debris disks. Future observations should test for common traits among these stars, such as stellar multiplicity and the existence of planets.

Support for GO-9475 was provided by NASA through a grant from STScI under NASA contract NAS5-26555.

REFERENCES

- Adams, F. C., & Laughlin, G. 2001, *Icarus*, 150, 151
 Ardila, D. R., et al. 2004, *ApJ*, 617, L147
 Augereau, J. C., Lagrange, A. M., Mouillet, D., Papaloizou, J. C. B., & Grorod, P. A. 1999, *A&A*, 348, 557
 Augereau, J. C., Nelson, R. P., Lagrange, A. M., Papaloizou, J. C. B., & Mouillet, D. 2001, *A&A*, 370, 447
 Aumann, H. H. 1985, *PASP*, 97, 885
 Burns, J. A., Lamy, P. L., & Soter, S. 1979, *Icarus*, 40, 1
 Decin, G., Dominik, C., Malfait, K., Mayor, M., & Waelkens, C. 2000, *A&A*, 357, 533
 Ida, S., Larwood, J., & Burkert, A. 2000, *ApJ*, 528, 351
 Kalas, P. 2005, *ApJ*, 635, L169
 Kalas, P., Graham, J. R., & Clampin, M. C. 2005, *Nature*, 435, 1067
 Kalas, P., & Jewitt, D. 1995, *AJ*, 110, 794
 ———. 1996, *AJ*, 111, 1347
 Kalas, P., Liu, M., & Matthews, B. 2004, *Science*, 303, 1990
 Kelsall, T., et al. 1998, *ApJ*, 508, 44
 Kenyon, S. J., & Bromley, B. C. 2004, *AJ*, 127, 513
 Krist, J. E., et al. 2005, *AJ*, 129, 1008
 Lachaume, R., Dominik, C., Lanz, T., & Habing, H. J. 1999, *A&A*, 348, 897
 Larwood, J. D., & Kalas, P. 2001, *MNRAS*, 323, 402
 Liou, J.-C., & Zook, H. A. 1999, *AJ*, 118, 580
 Mallik, S. V., Parthasarathy, M., & Pati, A. K. 2003, *A&A*, 409, 251
 Montes, D., et al. 2001, *MNRAS*, 328, 45
 Moro-Martín, A., & Malhotra, R. 2002, *AJ*, 124, 2305
 Nordstrom, B., et al. 2004, *A&A*, 418, 989
 Pantin, E., Lagage, P. O., & Artymowicz, P. 1997, *A&A*, 327, 1123
 Schneider, G., Silverstone, M. D., & Hines, D. C. 2005, *ApJ*, 629, L117
 Schneider, G., et al. 1999, *ApJ*, 513, L127
 Smith, B. A., & Terrile, R. J. 1984, *Science*, 226, 1421
 Song, I., Caillault, J.-P., Barrado y Navascues, D., Stauffer, J. R., & Randich, S. 2000, *ApJ*, 533, L41
 Stencel, R. E., & Backman, D. E. 1991, *ApJS*, 75, 905
 Strubbe, L. E., & Chiang, E. I. 2005, *ApJ*, submitted
 Thommes, E. W., Duncan, M. J., & Levison, H. F. 1999, *Nature*, 402, 635
 Trujillo, C. A., & Brown, M. E. 2001, *ApJ*, 554, L95
 Tsiganis, K., Gomes, R., Morbidelli, A., & Levison, H. F. 2005, *Nature*, 435, 459
 Zuckerman, B., & Song, I. 2004, *ApJ*, 603, 738